Effect of Microstructure on the Fracture Toughness of Polycrystalline Diamond and Polycrystalline Cubic Boron Nitride

Declan Carolan[1,a], Declan McNamara[1,b], Patricia Alveen[1,c], Neal Murphy[1,d] and Alojz Ivankovic[1,e]

[1] School of Mechanical and Materials Engineering, University College Dublin, Ireland

[a] declan.carolan@ucd.ie, [b] declan.mc-namara@ucdconnect.ie, [c] patricia.alveen@ucdconnect.ie, [d] neal.murphy@ucd.ie, [e] alojz.ivankovic@ucd.ie

Keywords: Brittle fracture, scale bridging, finite volume method, cohesive zone model

Abstract. Voronoi tessellation is employed to generate two-dimensional microstructures of single phase and dual interpenetrating phase materials. A novel finite volume based arbitrary crack propagation solver implemented in OpenFOAM is described. This solver allows for specification of different cohesive zone models for each phase within the microstructure as well as unique cohesive zone formulations at the interfaces of any material pair. Initial results suggest that the developed model is capable, at least qualitatively, of capturing the features of both inter-granular and trans-granular fracture.

Introduction

Over the past quarter century, both Polycrystalline Diamond (PCD) and Polycrystalline Cubic Boron Nitride (PCBN) have become the tool material of choice for both the oil and gas industry and high speed machining of aerospace alloys. PCD is used primarily in the oil and gas industry whereas PCBN is used for high speed machining of ferrous alloys. An ideal cutting tool material should be both hard and tough.

The mechanical performance of PCD and PCBN tools is significantly affected by their microstructure [1, 2]. The microstructure is often complex, consisting of grains of different sizes and morphologies as well as significant quantities of other phases. For this reason it is important to be able to accurately model a material microstructure. Early work by Ghosh and Yunshan [3] and Ghosh et al [4] developed a Voronoi cell finite element model (VCFEM). One should also refer to significant work by Espinosa and Zavattieri [5, 6] and Zhou and Zhai [7] who analysed dynamic fragmentation of ceramic composites by inserting cohesive elements along the grain boundaries. More recently, work by Zhou et al. [8] and Zhang et al. [9] have used Voronoi tessellation and embedded grain boundary cohesive elements to study inter-granular crack growth on a micro-structural level. Of particular note is work by Nittur et al. [10] who incorporated a procedure to handle the complex contact of fragmenting grains and fracture surfaces.

Microstructure Generation

Consider a pair of seed points, a and b, in $\mathbb{R}^2$ as shown in Figure 1. The perpendicular bisector of $\underline{ab}$ divides the plane into two halves. All points in the plane on one side of the perpendicular bisector are closer to a than to b, while all points on the opposite side of the perpendicular bisector are closer to b than to a. Next consider a third seed point, c. The perpendicular bisectors of $\underline{ac}$ and $\underline{bc}$ can be drawn as before. There are now three regions surrounding each seed point. Each region coincides at

the circumcentre of Δabc. Repeating this procedure divides $\mathbb{R}^2$ into a series of polygons known as a Voronoi diagram. A typical Voronoi Tessellation with 100 random seed points distributed randomly on the region $0 < x,y < 1$ is given in Figure 2. As Voronoi tessellation is defined on the entire plane, special care has to be taken with any seed points close to the boundary, which do not have sufficient neighbours to define a closed polygon.

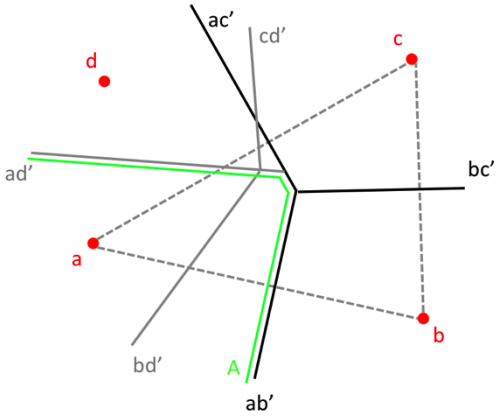

Fig. 1. Schematic showing the Voronoi tessellation of $\mathbb{R}^2$ into four regions.

In order to study the effect of grain size and distribution, Voronoi tessellation was used to generate random microstructures of both PCD and PCBN. First, the boundaries of the solution domain are specified. Next the nominal grain size and aspect ratio, i.e. columnar or equiaxed is chosen. The seeds are then distributed uniformly throughout the domain according to the previous choices. Each seed is then allowed to displace from the starting position according to a bounded random distribution. This ensures that no two seed points can get too close to each other and subsequently generate a final microstructure that is physically unrealistic. This also limits both the minimum and maximum grain size of the resultant microstructure. The degree of displacement of the seed points from the uniform seed arrangement is governed by two randomly distributed variables, a distance r, which is normally distributed and an angle θ, which is a uniformly distributed random variable between 0 and 2π. The resultant seed points are then used to obtain the Voronoi tessellation of the solution domain. The degree to which each point is allowed to deviate from the initial position, r, can be varied so as to control the regularity of the microstructure. Obviously points that are allowed to move a large distance from the initial position will generate an irregular microstructure with a large variance in grain area. Points that are constrained to remain close to the initial positions generate more regular microstructures. The effect of regularity of the final microstructure is shown in Fig. 2.

To generate an interpenetrating microstructure, the Voronoi tessellation is applied as before. As an additional step, each Voronoi tile is then reduced in area around the circumcentre of the tile until the desired area fraction of the second interpenetrating phase is met.

Finite Volume Method

Over the last number of years the Finite Volume (FV) method has become established as an alternative to the Finite Element Method for the solution of problems involving stress analysis. The method was first developed for the solution of solid mechanics problems by Demirdzic and co-workers [11–15]. Ivankovic and co-workers have applied the FV method successfully to the solution of both fracture problems [16–19] and fluid structure interaction problems [20, 21]. All of the

procedures and simulations in the current work were implemented and conducted using OpenFOAM-1.6-ext [22, 23].

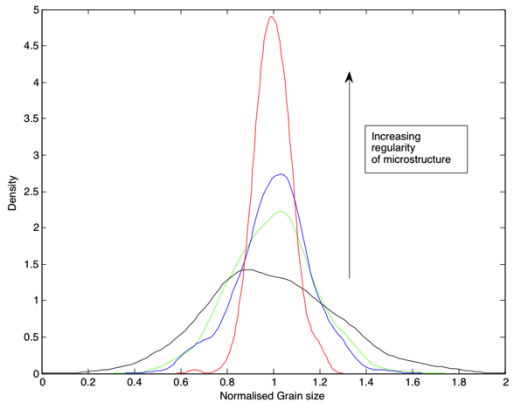

(a) Grain area density

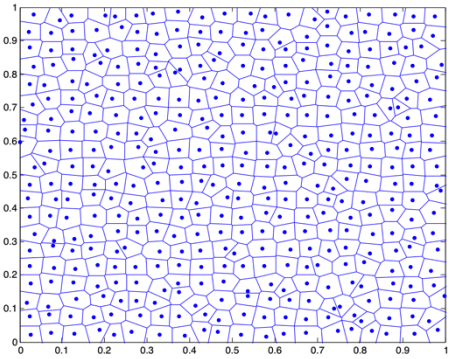

(b) Regular microstructure

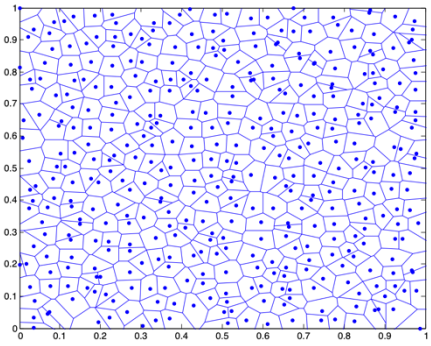

(c) Irregular Microstructure

Fig. 2. Effect of regularity on the grain size distribution of the final microstructure.

The arbitrary crack propagation model implemented allows prediction of crack propagation along internal control volume faces [24]. An internal control volume face at which the failure criterion is satisfied is turned into a pair of cohesive zone boundary faces. The traction force specified between these cohesive zone faces is governed by a cohesive zone model.

The cohesive zone model works on the basis that all the damage processes taking place locally ahead of the crack tip can be described by a unique stress-displacement relationship as shown in Fig. 3 (a). For the simplest models, two parameters are required to fully describe the model. These are the fracture energy G_{Ic} and the maximum cohesive strength σ_{max}. According to the cohesive zone model the traction between cohesive zone faces is a function of the separation distance between the faces. In case of mode I (opening) crack, only normal separation distance is considered and the traction-separation law defines normal cohesive traction between cohesive faces as a function of normal separation distance. An initially rigid general traction-separation law is shown in Fig. 3 (b). Once the critical traction, σ_{max} is reached, σ decreases from the critical traction to zero traction according to the specified traction-separation curve. When the critical normal separation δ_c is reached, fracture is assumed to have taken place and the cohesive faces are thereafter treated as traction-free faces.

Direct measurement of the shape of the cohesive law has proven to be very difficult, especially for brittle materials [25, 26]. Both Chandra et al. [27], Rots [28] and Murphy and Ivankovic [24] have

shown that when the damage stems from micro-cracking, the shape of the traction-separation law is important and typically a linear formulation describes these materials better than a Dugdale law.

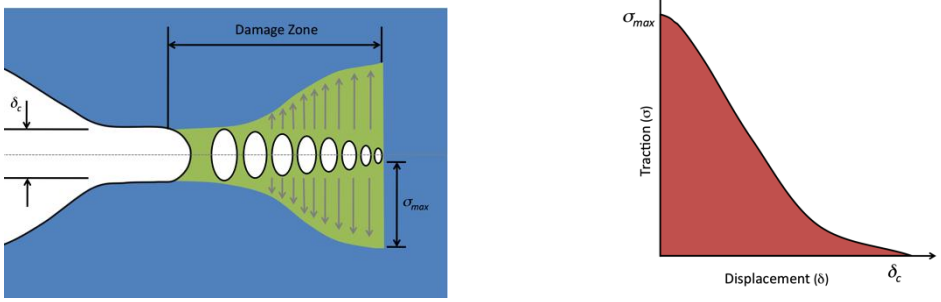

(a) Damage zone ahead of a growing crack (b) General form

Fig 3: Traction separation law

Results

Fig. 4 presents generated microstructures for four different starting grain sizes for a single phase material, typical of a polycrystalline diamond microstructure. Each microstructure is 100 μm by 100 μm. An initial notch has been incorporated into each microstructure of length 10 μm. A tensile load is applied by imposing a symmetric velocity at the top and bottom edges of the model.

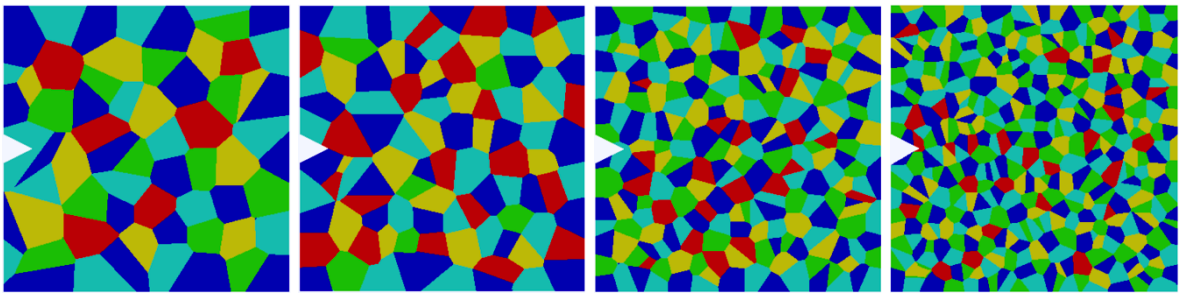

(a) d_{nom} = 12.5 μm (b) d_{nom} = 10 μm (c) d_{nom} = 6.7 μm (d) d_{nom} = 5 μm

Fig 4. Four different single phase SENT microstructures generated with different grain sizes, d_{nom}. The SENT specimen is 100 μm by 100 μm and the initial notch is 10 μm.

The crack path of each microstructure is given in Fig. 5. For the purposes of initial testing the grains were treated as elastic isotropic material with E = 800 GPa, ν = 0.12 and ρ = 3,000 kg/m^3. Cohesive properties of the grain was set to σ_{max} = 1,000 MPa and G_{Ic} = 100 J/m^2. Cohesive properties of the interface were set to be 60% of the grain properties, i.e. σ_{max} = 600 MPa and G_{Ic} = 60 J/m^2. The CZM shape was linear in all cases. This ensured that a degree of both trans-granular and inter-granular cracking would be observed. Each simulation was carried out in plane strain and only Mode I fracture was allowed. The loading rate was set to 0.01 mm/min, giving a strain rate of 1.7e-3 /sec.

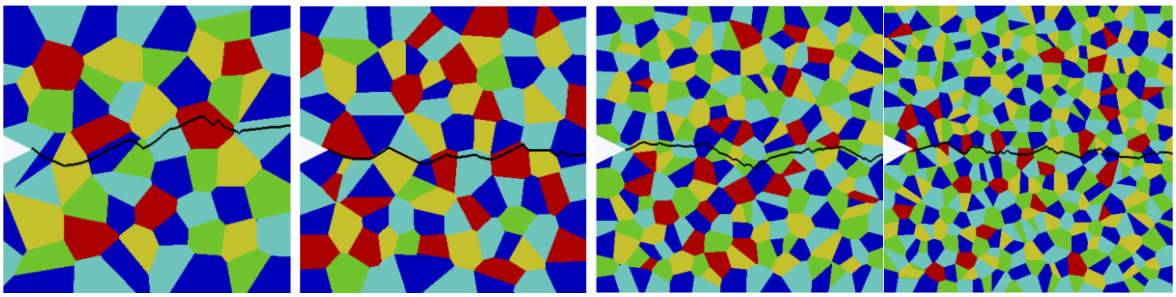

(a) d_{nom} = 12.5 μm (b) d_{nom} = 10 μm (c) d_{nom} = 6.7 μm (d) d_{nom} = 5 μm

Fig 5. Final crack paths of single phase microstructure

Fig. 6 presents the results of a fracture test on a dual phase microstructure, typical of PCBN microstructures. The elastic and cohesive properties of the grain are as before, while the elastic properties of the surrounding binder material are: E = 300 GPa, ν = 0.2 and ρ = 3,500 kg/m^3. The cohesive properties for the binder material and the interface are the same in this case, σ_{max} = 300 MPa and G_{Ic} = 100 J/m^2. This sample is loaded at both low rate, 1.7e-3 /sec, and high rate, 17 /sec. Multiple bifurcations of the main crack are observed at high rates. It is also of interest to note that there is not significant trans-granular cracking at the lower strain rate while many of the much stronger grains are cleaved at the higher rate of loading.

Fig. 7 is a scanning electron micrograph of the fracture surface of a PCBN material fractured in three point bend at a low strain rate. The notch tip is located at the bottom of the image and the crack propagation direction is towards the top of the image. The fracture is predominantly inter-granular and the crack path can be seen to be tortuous around the grains. This phenomenon is predicted quite well in Fig. 6. Fig. 8 presents a micrograph of the same PCBN material fractured at a high strain rate. Notch tip location and crack propagation direction are as before. There is significantly more transgranular cracking evidenced by the stepping of grains in the image. Additionally there is evidence of micro-cracking suggesting that secondary crack front may have occurred during the fracture process.

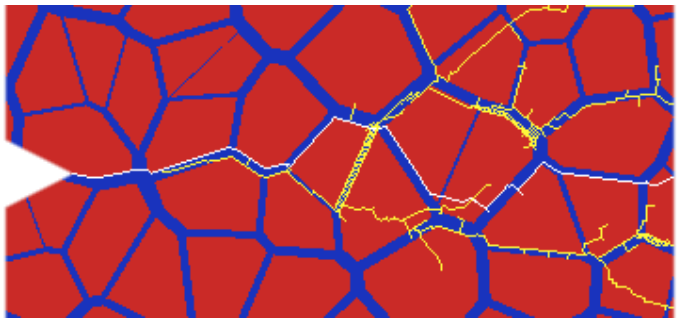

Fig 6. Crack paths in dual phase interpenetrating microstructure at low rate (white) and high rate (yellow). Bifurcation of the crack is observed at high strain rates.

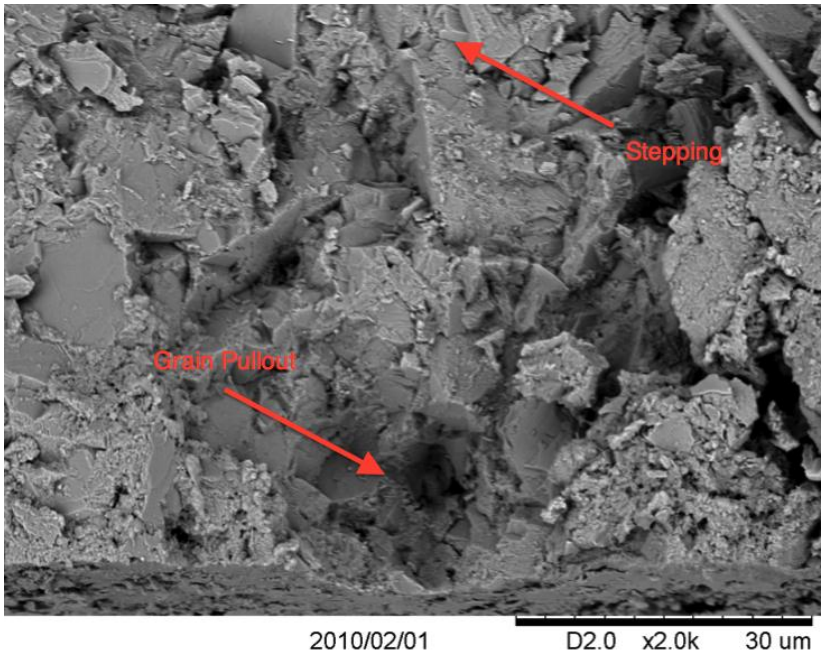

Fig 7. Typical fractograph of dual phase interpenetrating microstructure (PCBN) fractured at low rate. The fracture mode can be predominantly described as intergranular.

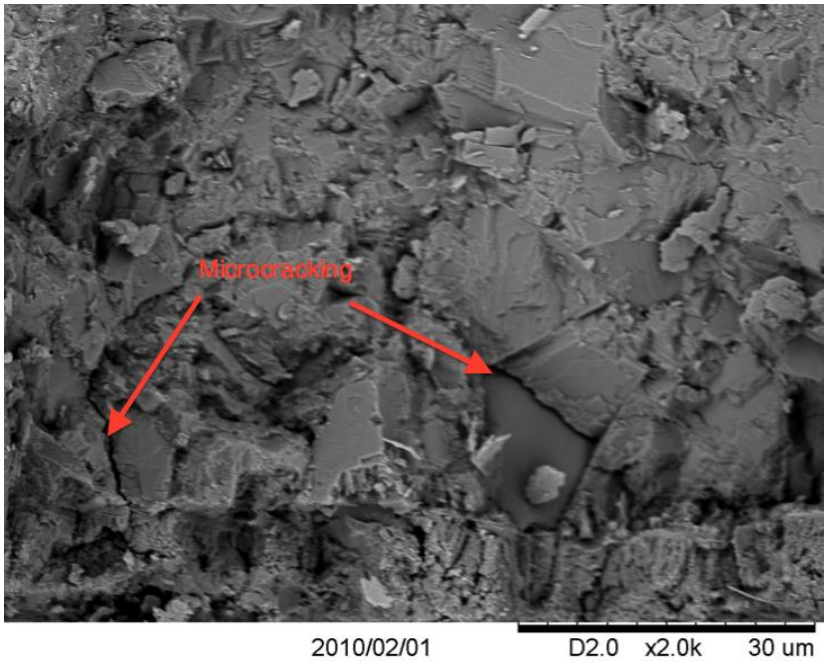

Fig 8. Typical fractograph of dual phase interpenetrating microstructure (PCBN) fractured at high rate. Both intergranular and transgranular fracture can be observed.

Conclusion

A technique based on work by previous researchers for generating statistically representative two-dimensional microstructures for a variety of materials has been presented. This technique can produce both single and multi-phase microstructures.

A multi-material crack propagation solver developed in OpenFOAM using the Finite Volume method was used to examine the fracture properties of a number of different microstructures. The

model was able to quantitatively predict both inter-granular and trans-granular fracture in both single phase and multi phase crystalline materials. The model was also able to predict crack bifurcation at higher rates of loading. The model predictions for a dual phase interpenetrating material agree with micrographs of fracture surfaces from experiment.
Future work will concentrate on extending the Voronoi tessellation method to 3-dimensions as well as refining the finite volume crack procedure to handle thermally initiated cracks.

References

[1] D. Carolan, P. Alveen, N. Murphy, A. Ivankovic, Effect of notch root radius on the fracture toughness of polycrystalline cubic boron nitride, Engineering Fracture Mechanics 78 (2011) 2885–2895.

[2] D. Carolan, N. Murphy, A. Ivankovic, Thermal shock resistance of polycrystalline cubic boron nitride, Journal of the European Ceramic Society, Available online at http://dx.doi.org/10.1016/j.jeurceramsoc.2012.03.013.

[3] S. Ghosh, L. Yunshan, Voronoi cell finite element model based on micropolar theory of thermoelasticity for heterogeneous materials, International Journal for Numerical Methods in Engineering 38 (1995) 1361– 1368.

[4] S. Ghosh, Z. Nowak, K. Lee, Tessellation based computational methods for the characterisation and analysis of heterogeneous microstructures, Composite Science and Technology 57 (1997) 1187–1210.

[5] P. Zavattieri, H. Espinosa, Grain level analysis of crack initiation and propagation in brittle materials, Acta Materiala 49 (2001) 4291-4311.

[6] H. Espinosa, P. Zavattieri, A grain level model for the study of failure initiation and evolution in polycrystalline brittle materials. Part I: Theory and numerical implementation, Mechanics of Materials 35 (2003) 333–364.

[7] J. Zhai, M. Zhou, Finite element analysis of micromechanical failure modes in a heterogeneous ceramic material system, International Journal of Fracture 101 (2000) 161–180.

[8] T. Zhou, C. Huang, H. Liu, J. Wang, B. Zou, H. Zhu, Crack propagation simulation in microstructure of ceramic tool materials, Computational Materials Science 54 (2012) 150–156.

[9] P. Zhang, M. Karimpour, D. Balint, J. Lin, D. Farrugia, A controlled poisson voronoi tessellation for grain and cohesive boundary generation applied to crystal plasticity analysis, Computational Materials Science, Available online at http://dx.doi.org/10.1016/j.commatsci.2012.02.022.

[10] P.G. Nittur, S. Maiti, P. Geubelle, Grain level analysis of dynamic fragmentation of ceramics under multi axial compression, Journal of the Mechanics and Physics of Solids 56 (2008) 993–1017.

[11] I. Demirdzic, D. Martinovic, A. Ivankovic, Numerical simulation of thermal deformation in welded specimens (in Croatian), Zavarivanje 31 (1988) 209–219.

[12] I. Demirdzic, D. Martinovic, Finite volume method for thermo-elasto- plastic stress analysis, Computer Methods in Applied Mechanics and Engineering 109 (1993) 331–349.

[13] I. Demirdzic, S. Muzaferija, Finite volume method for stress analysis in complex domains, International Journal for Numerical Methods in Engineering 37 (1994) 3751–3766.

[14] I. Demirdzic, S. Muzaferija, Numerical method for coupled fluid flow, heat transfer and stress analysis using unstructured moving meshes with cells of arbitrary topology, Computer methods in Applied Mechanics and Engineering 125 (1995) 235–255.

[15] I. Demirdzic, E. Dzaferovic, A. Ivankovic., Finite volume approach to thermoviscoelasticity, Numerical Heat Transfer, Part B 47 (3) (2005) 213–237.

[16] A. Ivankovic, I.Demirdzic, J. Williams, P. Leevers, Application of the finite volume method to

the analysis of dynamic fracture problems, In- ternational Journal of Fracture 66 (1994) 357–371.
[17] A. Ivankovic, I.Demirdzic, J. Williams, P. Leevers, Finite volume method and multigrid acceleration in modelling of rapid crack propagation in full-scale pipe test, Computational Mechanics 20 (1997) 46–52.
[18] A. Ivankovic, Finite volume modelling of dynamic fracture problems, Computer Modelling and Simulation in Engineering 4 (1999) 227–235.
[19] A. Ivankovic, K. Pandya, J. Williams, Crack growth predictions in polyethylene using measured traction-separation curves, Engineering Fracture Mechanics 71 (2004) 657–668.
[20] V. Kanyanta, A. Karac, A. Ivankovic, Validation of a fluid structure interaction numerical model for predicting flow transients in arteries, Journal of Biomechanics 42 (2009) 1705–1712.
[21] A. Karac, A. Ivankovic, Behaviour of fluid filled PE containers under impact: Theoretical and numerical investigation, International Journal of Impact Engineering 36 (2009) 621–631.
[22] H. Weller, G. Tabor, H. Jasak, C. Fureby, A tensorial approach to CFD using object oriented techniques, Computers in Physics 12 (1998) 620– 631.
[23] OpenFOAM, www.wikki.co.uk, www.openfoam.co.uk (2011).
[24] N. Murphy, A. Ivankovic, The prediction of dynamic fracture evolution in PMMA using a cohesive zone model, Engineering Fracture Mechanics 72 (2005) 861–875.
[25] M. Elices, G. V. Guinea, J. Gomez, J. Planas, The cohesive zone model: Advantages, limitations and challenges, Engineering Fracture Mechanics 69 (2002) 137–163.
[26] R. de Borst, Numerical aspects of cohesive-zone models, Engineering Fracture Mechanics 70 (2003) 1743–1757.
[27] N. Chandra, H. Li, G. Shet, H. Ghonem, Some issues in the application of cohesive zone models for metal ceramic interfaces, International Journal of Solids and Structures 39 (2002) 2827–2855.
[28] J. Rots, Strain-softening analysis of concrete fracture specimens, in: F. Wittmann (Ed.), Fracture toughness and fracture energy of concrete, Elsevier Science, Amsterdam, 1986, pp. 137–148.

Acknowledgements
The authors would like to acknowledge the financial support of Enterprise Ireland, The Irish Research Council for Science Engineering and Technology and Element Six Limited. The authors gratefully acknowledge Dr. Zeljko Tukovic, FSB, Univeristy of Zagreb, Croatia for helpful discussion.